Available online at www.sciencedirect.com
ScienceDirect
Polymer 48 (2007) 579–589
polymer
www.elsevier.com/locate/polymer

Molecular relaxation in cross-linked poly(ethylene glycol) and poly(propylene glycol) diacrylate networks by dielectric spectroscopy

Sumod Kalakkunnath [a], Douglass S. Kalika [a,*], Haiqing Lin [b,1], Roy D. Raharjo [b], Benny D. Freeman [b]

[a] Department of Chemical and Materials Engineering and Center for Manufacturing, University of Kentucky, 177 Anderson Hall (Tower), Lexington, KY 40506-0046, United States
[b] Center for Energy and Environmental Resources, Department of Chemical Engineering, University of Texas at Austin, Austin, TX 78758, United States

Received 9 October 2006; received in revised form 21 November 2006; accepted 22 November 2006
Available online 13 December 2006

Abstract

The molecular relaxation characteristics of rubbery amorphous crosslinked networks based on poly(ethylene glycol) diacrylate [PEGDA] and poly(propylene glycol) diacrylate [PPGDA] have been investigated using broadband dielectric spectroscopy. Dielectric spectra measured across the sub-glass transition region indicate the emergence of an intermediate ''fast'' relaxation in the highly crosslinked networks that appears to correspond to a subset of segmental motions that are more local and less cooperative as compared to those associated with the glass transition. This process, which is similar to a distinct sub-T_g relaxation detected in poly(ethylene oxide) [PEO], may be a general feature in systems with a sufficient level of chemical or physical constraint, as it is observed in the crosslinked networks, crystalline PEO, and PEO-based nanocomposites.

Keywords: Membranes; Poly(ethylene oxide); Dielectric spectroscopy

1. Introduction

The formulation of gas separation membranes for the selective removal of CO_2 from mixtures with light gases such as H_2 or CH_4 is an area of growing interest, as such membranes would be useful for a number of high-volume industrial applications [1]. In particular, membranes specifically formulated to engender high CO_2 permeability and high CO_2/light gas selectivity could be used for the removal and potential sequestration of CO_2 as low-pressure permeate, with the light gas components retained at or near feed pressure for subsequent transport or use. Recently, rubbery polymeric membranes based on crosslinked poly(ethylene oxide) [PEO] have been the subject of extensive study for the preferential removal of CO_2 from gas mixtures. Neat (*i.e.* uncrosslinked) PEO exhibits favorable selectivity for CO_2 over non-polar light gases owing to quadrupole–dipole interactions between the CO_2 penetrant molecules and the ethylene oxide units that constitute the polymer chain backbone [2,3]. PEO, however, has a strong tendency to crystallize, which limits the bulk permeability that can be achieved with the homopolymer. As such, a number of approaches have been explored to reduce or eliminate crystallinity in PEO and related materials, while at the same time maintaining the polar character of the polymer matrix to ensure high CO_2 selectivity. The introduction of chemical crosslinks, for example, can be used to suppress crystallization in PEO. When the number of ethylene oxide segments between crosslink junctions is limited to approximately 20 or less, fully amorphous networks can be obtained [4].

The synthesis of highly permeable, CO_2-selective membranes based on the ultraviolet (UV) photopolymerization of poly(ethylene glycol) [PEG] and poly(propylene glycol) [PPG] diacrylates has been investigated in our laboratories

* Corresponding author. Tel.: +1 859 257 5507; fax: +1 859 323 1929.
E-mail address: kalika@engr.uky.edu (D.S. Kalika).
[1] Present address: Membrane Technology and Research, Inc., 1360 Willow Road, Suite 103, Menlo Park, CA 94025.

0032-3861/$ - see front matter © 2006 Elsevier Ltd. All rights reserved.
doi:10.1016/j.polymer.2006.11.046

as a route to produce amorphous, rubbery crosslinked polymer networks with optimum transport properties [5–13]. In these studies, diacrylate crosslinkers were copolymerized with mono-functional PEG and PPG acrylates in an effort to tailor the network architecture, free volume, and gas separation characteristics of the resulting membranes. The viscoelastic relaxation properties of the networks were examined in detail using dynamic mechanical analysis, with a goal of elucidating the relationships between network structure, crosslink density and polymer chain dynamics as they pertain to gas separation performance [7,8,13]. In the course of this work, it became evident that relatively small changes in the details of the network structure or composition (*e.g.* variations in pendant terminal groups) could have a significant impact on segmental dynamics, fractional free volume, and corresponding permeability and selectivity.

In the present study, we report on the dielectric relaxation characteristics of amorphous polymer networks prepared by the photopolymerization of poly(ethylene glycol) diacrylate [PEGDA] and poly(propylene glycol) diacrylate [PPGDA]. Broadband dielectric spectroscopy is a sensitive and non-intrusive method for probing motional relaxations in polymeric solids over a wide range of temperature and timescale, and has been used to investigate relaxations in a variety of polymeric materials including semi-crystalline polymers and blends [14] as well as crosslinked polymer networks [15]. For the polymer networks in this study, we are interested in the influence of crosslinks on the measured dielectric relaxation characteristics across both the sub-glass and glass–rubber transition regions. In general, the presence of high levels of crosslinking in polymeric networks results in a restriction of segmental mobility in the vicinity of the crosslink junctions that reduces the conformational freedom of the polymer chains, often leading to an increase in the measured glass transition temperature and inhomogeneous broadening of the glass–rubber relaxation [16–18]. This broadening reflects the range of relaxation environments experienced by the responding dipoles and the constraint imposed by the presence of the crosslinks. As will be demonstrated for the non-crystalline networks studied here, the constraints that are present in the crosslinked polymer lead to dielectric relaxation characteristics that are in many respects analogous to features encountered upon the relaxation of constrained amorphous segments in crystalline PEO [19] as well as amorphous PEO confined at the nanometer scale in intercalated nanocomposites [20,21].

2. Experimental

2.1. Materials

Poly(ethylene glycol) diacrylate [PEGDA; nominal MW = 700 g/mol] and poly(propylene glycol) diacrylate [PPGDA; nominal MW = 900 g/mol] crosslinkers, as well as poly(ethylene oxide) polymer [PEO; reported $M_v = 1{,}000{,}000$], were obtained from Aldrich Chemical Company (Milwaukee, WI). 1-Hydroxyl-cyclohexyl phenyl ketone [HCPK] initiator was also purchased from Aldrich. The PEGDA and PPGDA molecular weights were characterized using proton nuclear magnetic resonance (^{1}H NMR) and fast atom bombardment mass spectrometry (FAB-MS) in order to verify the values provided by the supplier; details of these characterizations have been reported previously [5,13]. For PEGDA, the number average molecular weight values determined by ^{1}H NMR and FAB-MS were 743 and 730 g/mol, respectively, corresponding to a monomeric repeat value for the crosslinker, $n \sim 14$. For PPGDA, the number average molecular weight values determined by ^{1}H NMR and FAB-MS were 809 and 822 g/mol, respectively. These values correspond to a monomeric repeat length, $n \sim 12$.

2.2. Polymer film preparation

Crosslinked polymer films based on 100% diacrylate (*i.e.*, PEGDA or PPGDA) were prepared by UV photopolymerization. A pre-polymer solution comprised of the liquid crosslinker and 0.1 wt% HCPK was sandwiched between two quartz plates, which were separated by spacers to control film thickness. The mixture was polymerized by exposure to 312 nm UV light in a UV Crosslinker (Model FB-UVXL-1000, Fisher Scientific) for 90 s at 3 mW/cm^2. The solid films obtained by this process were three-dimensional networks and contained a negligible amount of low molecular weight polymer (*i.e.*, sol) that was not bound to the network. In order to remove any residual sol or unreacted crosslinker, the films were washed with toluene in a Soxhlet extractor (Chemglass) for 1 day. Film thickness for the crosslinked networks was approximately 350 μm; the precise thickness for each film was measured using a digital micrometer readable to ±1 μm.

The extent of the polymerization reaction in the crosslinked polymer films was determined using FTIR-ATR spectroscopy (Nexus 470 spectrometer from Thermo Nicolet, Madison, WI). The reaction of the acrylate double bonds during polymerization leads to a decrease in the intensity of sharp peaks at 810 cm^{-1} (ascribed to the twisting vibration of the acrylic CH_2=CH bond), at 1410 cm^{-1} (deformation of the CH_2=CH bond) and at 1190 cm^{-1} (acrylic C=O bond) [22,23]. For both the PEGDA [5] and PPGDA [13] networks, FTIR-ATR spectra showed essentially complete disappearance of the characteristic double bond peaks, indicating that the reaction conversion was close to 100%. In addition, spectra taken from opposite sides of the individual polymer films were virtually identical, suggesting that full reaction was achieved throughout each network, with no variation as a function of film depth.

PEO films were obtained by solution casting according to the method detailed in Ref. [2]. PEO powder (3 wt%) was dissolved in distilled water and cast into flat-bottomed Petri dishes. The incipient films were covered in order to control the rate of drying, and were allowed to dry slowly under ambient conditions until a uniform film was obtained. All films were then held under vacuum at room temperature until further characterization. The thickness of the PEO films was ~500 μm. Crystallinity in the films was evaluated using differential scanning calorimetry (Perkin–Elmer DSC-7): sample size was approximately 10 mg, and a heating rate of 10 °C/min was used.

2.3. Dielectric relaxation spectroscopy

Dielectric spectroscopy measurements were performed using the Novocontrol Concept 40 broadband dielectric spectrometer (Hundsangen, Germany). In order to ensure the integrity of electrical contact during measurement, concentric silver electrodes (33 mm diameter) were vacuum evaporated on each polymer sample using a VEECO thermal evaporation system. Samples were then mounted between gold platens and positioned in the Novocontrol Quatro Cryosystem. All samples were rigorously dried under vacuum prior to measurement and sample mounting procedures were designed to minimize exposure to ambient moisture. Dielectric constant (ε') and loss (ε'') were recorded in the frequency domain (0.1 Hz to 1.0 MHz) at discrete temperatures from −150 °C to 100 °C.

3. Results and discussion

3.1. Properties of XLPEGDA, XLPPGDA, PEO films

UV photopolymerization of the PEGDA and PPGDA diacrylate crosslinkers, as described above, results in amorphous, rubbery polymer networks with essentially 100% conversion of the diacrylate end groups as confirmed by FTIR-ATR. An idealized schematic of the PEGDA network is shown in Fig. 1. Characteristics of the crosslinked networks as determined by calorimetry, dynamic mechanical analysis and density measurement are reported in Table 1 [5,7,13]. In these fully reacted networks, the effective crosslink density (and average molecular weight between crosslinks, M_c) is established by the molecular weight of the diacrylate pre-polymer: for PEGDA ($n = 14$), $M_c = 688$ g/mol, while for PPGDA ($n = 12$), $M_c = 768$ g/mol. Both networks display very similar glass transition temperatures, but the density of the crosslinked PPGDA [XLPPGDA] is approximately 10% lower than that of crosslinked PEGDA [XLPEGDA]. This difference in bulk density is reflected in the estimation of fractional free volume

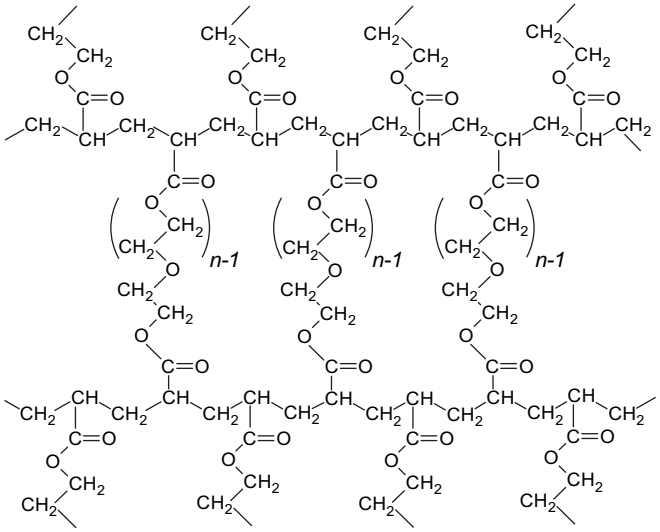

Fig. 1. Idealized network schematic for crosslinked 100% PEGDA.

Table 1
Characteristics of XLPEGDA and XLPPGDA networks

	T_g (DSC), °C	T_α (DMA)[a], °C	Density (g/cm^3)	FFV
XLPEGDA [5,7]	−40	−35	1.183	0.118
XLPPGDA [13]	−43	−37	1.065	0.160

[a] Based on maximum in dynamic mechanical tan δ, 1 Hz (see Ref. [7]).

(FFV) for the two networks, with FFV = 0.160 for XLPPGDA, and FFV = 0.118 for XLPEGDA. Details on the determination of FFV for the networks are provided in Refs. [5] and [13].

PEO films prepared by solution casting were characterized using DSC, and showed properties close to those previously reported by Lin and Freeman [2]. For the samples studied here, DSC thermograms indicated a melting peak temperature of 68 °C, and a percentage crystallinity of ~80 wt% based on the 100% crystal heat of fusion reported by Wunderlich [24].

3.2. Dielectric results for XLPEGDA, XLPPGDA, PEO films

Dielectric results for the crosslinked film based on 100% PEGDA are shown in Fig. 2 as dielectric constant (ε') and dielectric loss (ε'') *vs.* temperature at frequencies ranging

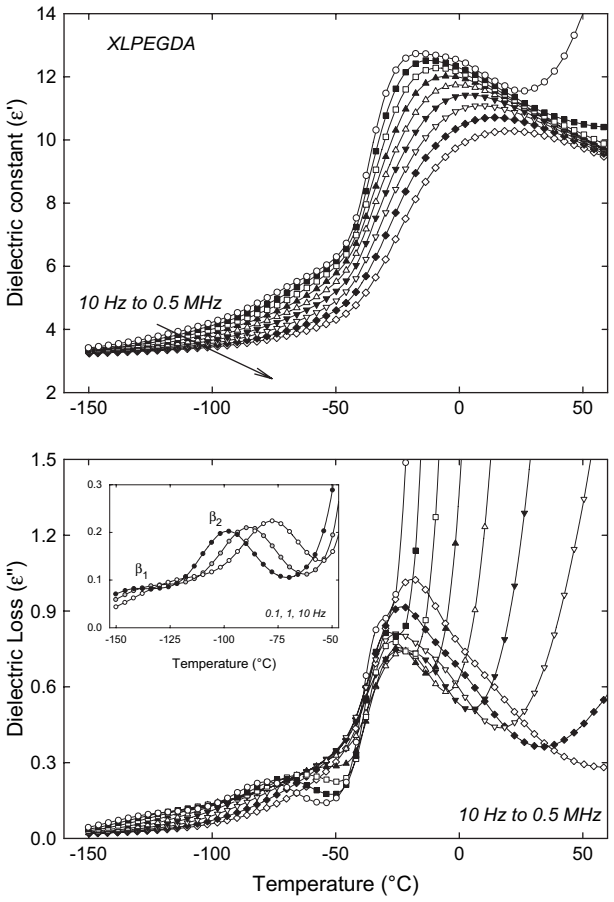

Fig. 2. Dielectric constant (ε') and loss (ε'') *vs.* temperature for XLPEGDA; selected frequencies from 10 Hz to 0.5 MHz. *Inset*: expanded view of dielectric loss across the sub-glass region at 0.1 Hz (●), 1 Hz (◍), and 10 Hz (○).

from 10 Hz to 0.5 MHz. An expanded plot of dielectric loss at frequencies of 0.1, 1, and 10 Hz is also provided for the sub-glass region (see inset). The data show two apparent dipolar relaxation processes with increasing temperature as evidenced by the overlapping, incremental increases in dielectric constant and corresponding peaks in dielectric loss. These processes are designated as the β and α relaxations, respectively, with the higher-temperature α relaxation corresponding to the large-scale segmental motions associated with the glass transition. In the sub-glass region, lower-frequency measurements show that the β relaxation is comprised of two distinct processes, which are designated as the β_1 (lower temperature) and β_2 (higher temperature) relaxations, respectively. The strong increase in dielectric loss at low frequencies and high temperatures (*i.e.*, above the glass transition) reflects the onset of conduction associated with the transport of mobile charge carriers in the rubbery amorphous matrix [25].

Fig. 3 shows three-dimensional relaxation contour maps for XLPEGDA, XLPPGDA, and crystalline PEO. In each case, the data are plotted as dielectric loss *vs.* temperature *vs.* frequency. For all three materials, we observe two distinct relaxation processes in the sub-glass region (designated as β_1 and β_2); these relaxations merge with increasing frequency, with the combined β process eventually merging with the (glass–rubber) α relaxation at the highest frequencies measured. The influence of conduction is evident on the far left of each plot, as dielectric loss increases strongly with temperature. Conduction effects are especially prominent in the PEO sample as the presence of internal crystal boundaries results in local charge blocking and an additional contribution to the overall polarization (Maxwell–Wagner–Sillars (MWS) polarization).

In order to interpret the dielectric results for the crosslinked networks, it is useful to examine previous reports of dielectric relaxation properties for the appropriate uncrosslinked analogs, *i.e.* PEO and poly(propylene oxide) [PPO]. Earlier studies on the dielectric and dynamic mechanical relaxation of PEO indicate a total of three relaxation processes [26–31]: a high-temperature local process originating in the crystalline phase, a cooperative segmental process occurring in non-crystalline regions and usually correlated with the glass transition, and a local low-temperature twisting process, also associated with the non-crystalline phase. Various labeling conventions have been adopted for these motional processes, with the high-temperature crystalline process typically designated as the α (or α_c) process, and the glass transition and local sub-glass processes designated as β and γ, respectively [32,33]. Recent broadband dielectric measurements reported by Jin et al. reveal an additional local process situated between the β and γ relaxations, designated γ′ [19]. Based on the characteristics of the relaxation, Jin and co-workers proposed that the distinct γ′ process corresponds to segmental motions occurring in the crystal–amorphous order–disorder transition region, in the vicinity of the crystal lamellar surface. In our PEO studies (see Fig. 3c), two sub-glass relaxations are also clearly seen, with the intermediate transition designated as the β_2 relaxation according to the labeling convention adopted for the XLPEGDA and XLPPGDA networks. The position of the β_2

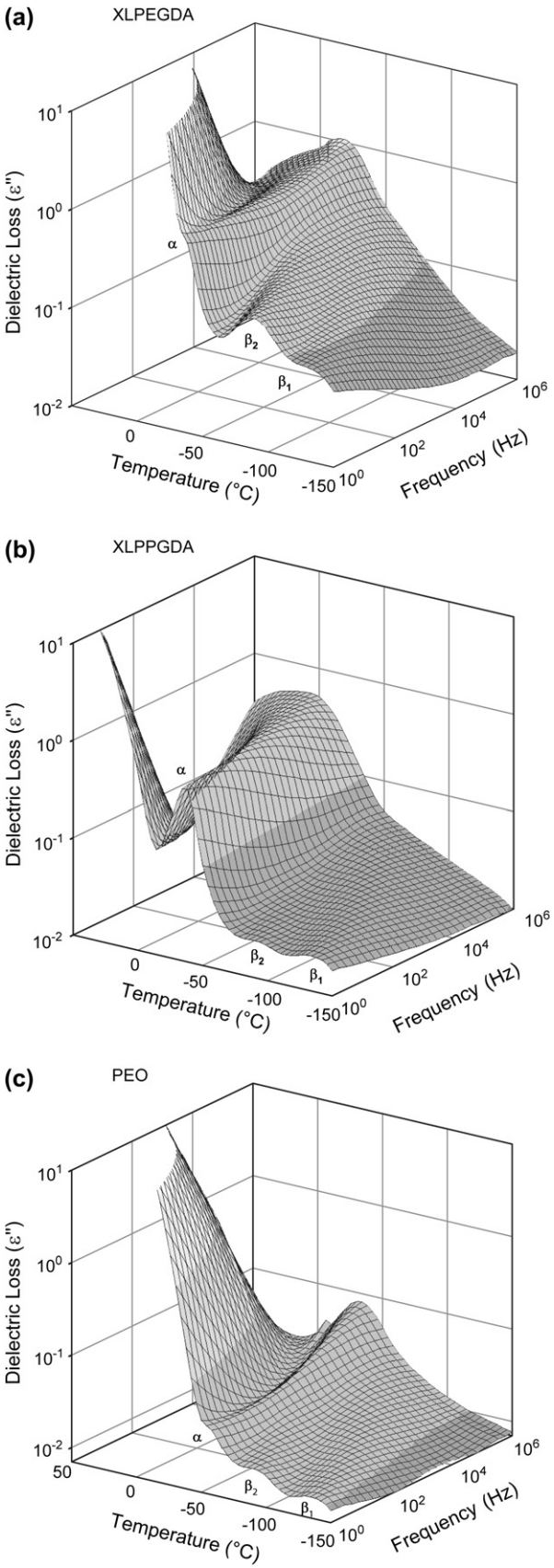

Fig. 3. Contour plot of dielectric loss (ε″) *vs.* temperature (°C) *vs.* frequency (Hz). (a) XLPEGDA; (b) XLPPGDA; (c) PEO.

relaxation in our PEO data is virtually the same as that reported by Jin et al. Notably, both of the amorphous crosslinked networks also show an intermediate (β_2) relaxation. The origin of this relaxation in the networks, and its relation to the process observed in crystalline PEO, is discussed below.

The dielectric relaxation characteristics of amorphous poly(propylene glycol) and poly(propylene oxide) in the glassy and liquid states have been measured by a number of investigators [34–42]. PPO displays two dielectric relaxation processes in the vicinity of T_g: a fast (lower temperature) process reflecting the segmental motions associated with the glass–rubber transition, and a slow (higher temperature) process corresponding to normal mode re-orientations that are detected owing to the presence of a cumulative dipole moment along the polymer chain. These relaxations are designated as the α and α' (or α_N) processes, respectively. In the glassy state, two sub-glass relaxations are detected, designated as the γ and β processes [37]. In the PPO polymer, the lower-temperature γ relaxation is only observed at temperatures below −150 °C. A number of dielectric studies have examined the influence of molecular weight on the characteristics of the normal mode motions as well as on the relationship between the β and α relaxations [35,38,40,41]. For low molecular weight PPG oligomers, the β and α relaxations overlap to a significant degree, and a distinct β relaxation is difficult to distinguish. At higher (*i.e.* polymeric) molecular weights, the sub-glass relaxation shifts to shorter relaxation times relative to the α process, and a more distinct β peak emerges. In all cases, however, the intensity of the β process remains at least 1 order of magnitude below that of the glass–rubber relaxation. Comparison of the β and α peaks for XLPPGDA (Fig. 3b) reveals a similar result with respect to relaxation intensity.

3.3. Analysis of sub-glass relaxations

For all three materials examined (XLPEGDA, XLPPGDA, PEO), there is considerable overlap of the dielectric relaxations in the sub-glass region. In order to establish the characteristics of each individual process, the data were fit in the frequency domain according to a dual Havriliak–Negami (HN) model [43,44]:

$$\varepsilon^* = \varepsilon' - i\varepsilon'' = \varepsilon_{U_1} + \sum_{i=1}^{2} \frac{\varepsilon_{R_i} - \varepsilon_{U_i}}{\left[1 + (i\omega\tau_{HN_i})^{a_i}\right]^{b_i}} \quad (1)$$

where ε_R and ε_U represent the relaxed ($\omega \to 0$) and unrelaxed ($\omega \to \infty$) values of the dielectric constant for each individual relaxation, $\omega = 2\pi f$ is the frequency, τ_{HN} is the relaxation time for each process, and a and b represent the broadening and skewing parameters, respectively. All curve fits reported here were obtained using the WinFIT software package provided with the Novocontrol dielectric spectrometer. For the sub-glass relaxations (β_1 and β_2), it was observed that satisfactory fits to the dielectric dispersion could be obtained with the skewing parameter (b) set equal to 1 in all cases; this corresponds to the symmetric Cole–Cole form of Eq. (1) [45].

A representative dual HN curve fit for XLPEGDA in the β relaxation region is shown in Fig. 4. The data are plotted as dielectric loss *vs.* frequency at a measurement temperature of −78 °C. When plotted on this basis, the lower-temperature β_1 relaxation appears on the right side, and the higher-temperature β_2 relaxation appears on the left; the individual relaxation fits are indicated by the dashed lines. Dielectric loss data and corresponding HN fits for the entire dual-relaxation region are plotted in Fig. 5. Across this range, the overall

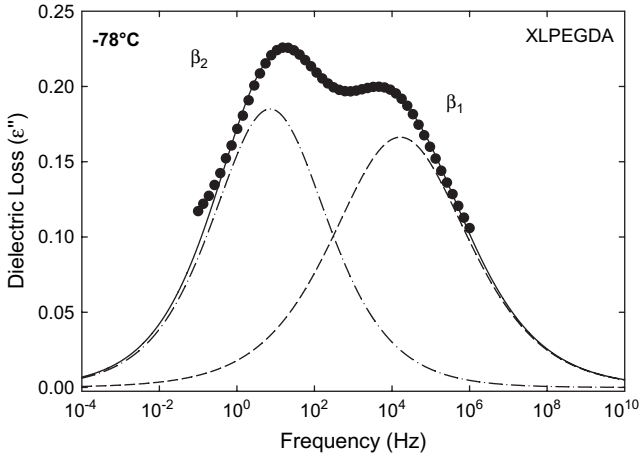

Fig. 4. Dielectric loss (ε'') *vs.* frequency (Hz) for XLPEGDA at −78 °C. Solid curve is dual HN fit; dashed curves are individual HN fits for the β_1 and β_2 relaxations.

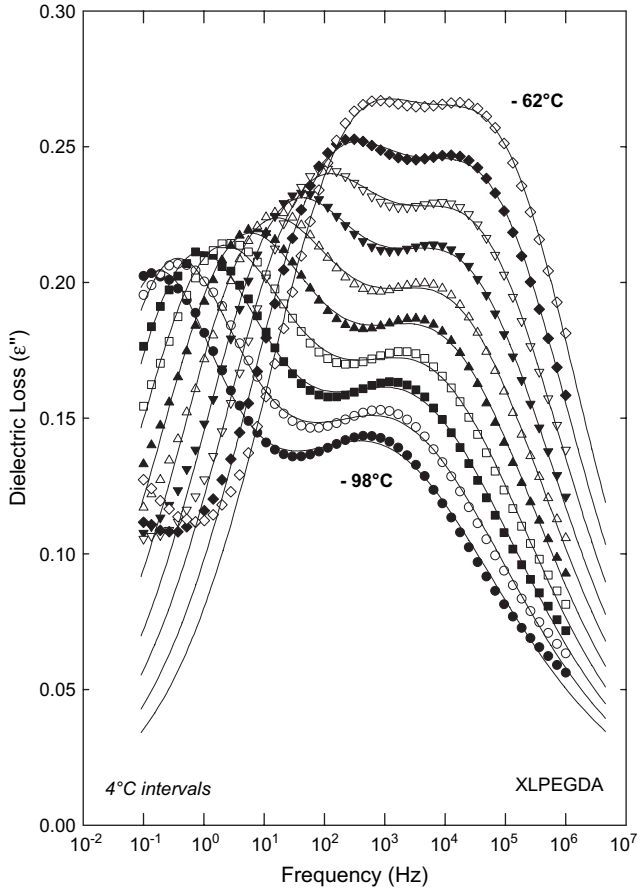

Fig. 5. Dielectric loss (ε'') *vs.* frequency (Hz) for XLPEGDA; temperatures from −98 °C to −62 °C at 4 °C intervals. Solid curves are dual HN fits.

relaxation intensity is observed to increase with increasing temperature, and the relaxations eventually merge at higher temperatures. In the case of XLPEGDA, deconvolution of the two relaxations could be reasonably accomplished at temperatures up to −62 °C. At the higher temperatures shown in Fig. 5, the influence of the glass–rubber (α) relaxation appears at low frequencies.

A comparison of the sub-glass dielectric relaxation response for XLPEGDA, XLPPGDA and PEO (−78 °C) is shown in Fig. 6. For each of the three polymers, overlapping β_1 and β_2 relaxations are observed. The peak positions (and corresponding relaxation times) associated with these transitions are nearly the same in all three materials. When comparing the dielectric relaxation intensity associated with these polymers, it is necessary to consider the composition of each material as well as its morphology. In crosslinked PEGDA, the network is 100% amorphous (as confirmed previously by DSC and X-ray [5]), in contrast to PEO, which is ~80% crystalline. For sub-glass relaxations that originate in non-crystalline regions of the PEO polymer, a significant fraction of the PEO segments will be incapable of responding to the applied alternating field, and thus will not contribute to the measured dielectric response. In addition, the presence of (−COO−) ester groups at the crosslink junctions in XLPEGDA and XLPPGDA increases the overall concentration of dipoles in these materials as compared to PEO or PPO, with the potential to thereby increase the net dielectric intensity of the observed relaxations.

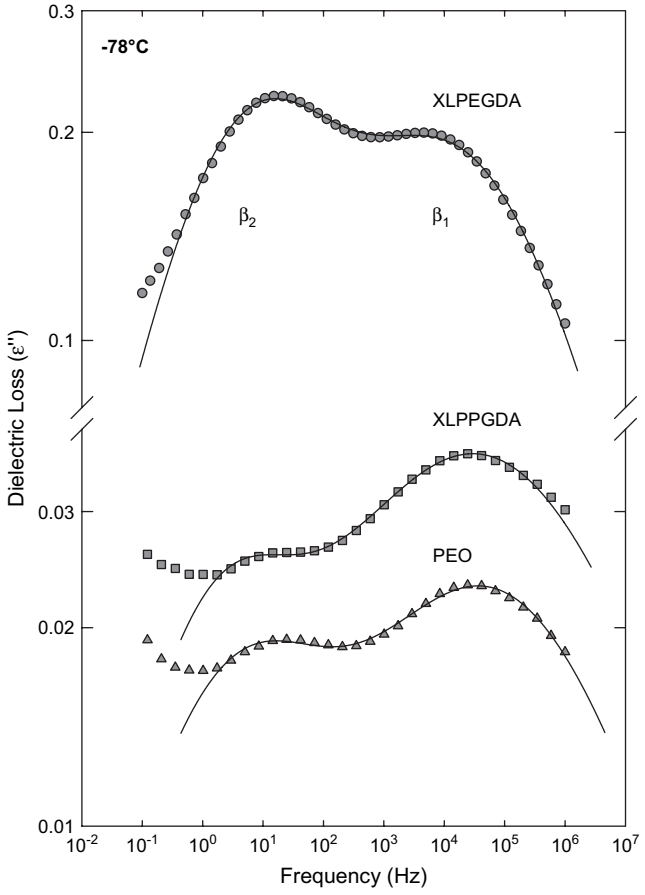

Fig. 6. Dielectric loss (ε'') *vs.* frequency (Hz) for XLPEGDA, XLPPGDA and PEO at −78 °C. Solid curves are dual HN fits.

Examination of the sub-glass relaxation response for XLPEGDA *vs.* PEO in Fig. 6 shows an approximately 1 order of magnitude lower dielectric relaxation intensity for crystalline PEO, as compared to XLPEGDA. As discussed above, this difference is attributable largely to the high fraction crystallinity in the PEO polymer as well as the potential additional contribution of the ester dipoles present in the XLPEGDA network. However, the respective β_1 and β_2 relaxation times ($\tau_{MAX} = [2\pi f_{MAX}]^{-1}$) are virtually identical for both XLPEGDA and PEO, so these motional processes could very well have the same or similar molecular origin.

Comparison of the sub-glass relaxations for XLPEGDA *vs.* XLPPGDA in Fig. 6 shows that the relaxation intensity for XLPPGDA is much lower than that observed for XLPEGDA (see also Fig. 3). The intensity of a particular dielectric relaxation depends on a number of factors, perhaps most fundamentally on the concentration of dipoles available that could potentially re-orient in response to an applied alternating field. An accounting of the differences in molar mass and density for the two crosslinked networks indicates that the number of ether linkages in the XLPPGDA network is 70% the number present in the XLPEGDA network, and that the XLPPGDA network contains 81% the number of −COO− groups present in XLPEGDA. Clearly, these values are not sufficient to explain the observed difference in sub-glass relaxation intensity for the two networks. In addition to differences in dipolar concentration, structural factors will influence the measured dielectric intensity, as conformational constraints and possible dipolar cancellations typically lead to relaxation intensities that are well below what would be expected based on a full and uncorrelated dipolar response. The relatively low intensity of the sub-glass relaxation in XLPPGDA is consistent with the observed dielectric response in PPO [37,40,41]. Apparently, the presence of the dipolar ester units in the XLPPGDA network does not alter this qualitative result, either when considering the relative intensity of the β and α relaxations in XLPPGDA or when comparing the sub-glass relaxation intensities in XLPPGDA *vs.* XLPEGDA.

The application of dual HN curve fits across the sub-glass region provides for the determination of dielectric relaxation intensity ($\Delta\varepsilon = \varepsilon_R - \varepsilon_U$), relaxation time ($\tau_{HN}$), and broadening parameter (a) for the individual β_1 and β_2 relaxations. Fig. 7 shows the results for XLPEGDA, XLPPGDA, and PEO. For the β_1 process, relaxation intensity is nearly independent of temperature, while for the β_2 process, $\Delta\varepsilon$ increases with temperature for XLPEGDA. Examination of the broadening parameter as a function of temperature reveals opposing trends for the β_1 and β_2 relaxations in all three materials. For the β_1 process, the symmetric dispersion is observed to narrow with increasing temperature (*i.e.*, the value of the broadening parameter increases). This result, which reflects a narrower distribution of relaxation times with increasing thermal energy, is consistent with the trend observed for both sub-glass and glass–rubber transitions in many common polymers

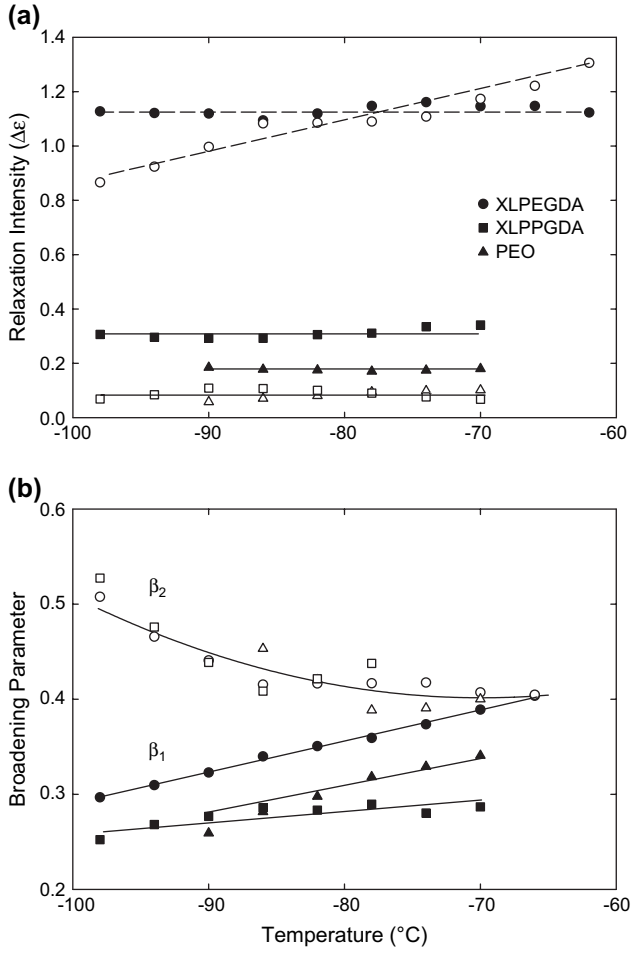

Fig. 7. HN curve fit parameters for XLPEGDA, XLPPGDA and PEO *vs.* temperature (°C). (a) Relaxation intensity; (b) HN broadening parameter. Filled symbols correspond to the β_1 relaxation; unfilled symbols correspond to the β_2 relaxation.

[46]. For the β_2 process, however, the relaxation is observed to broaden with increasing temperature. This behavior, while unusual, has been reported previously for the γ' process in crystalline PEO, a relaxation that was assigned to localized motions originating in the crystal–amorphous order–disorder transition region. Jin et al. [19] speculated that the broadening of the γ' relaxation in PEO was the result of "environmental asymmetry" between the amorphous phase, which becomes more mobile with increasing temperature, and the crystalline phase, which remains immobile. Consequently, the responding dipoles located in the order–disorder transition region experience a more heterogeneous relaxation environment at higher temperatures, leading to a broader dispersion. It appears that a similar situation exists in the XLPEGDA and XLPPGDA networks, where the crosslink junctions remain relatively rigid with increasing temperature, resulting in a net increase in dispersion breadth across the β_2 relaxation.

The time–temperature characteristics for the β_1 and β_2 relaxations are presented in an Arrhenius plot of $\log(f_{MAX})$ *vs.* $1000/T$(K) in Fig. 8. For the symmetric sub-glass processes, f_{MAX} was determined directly from the individual HN curve fits. Both the β_1 and β_2 transitions show a linear, Arrhenius

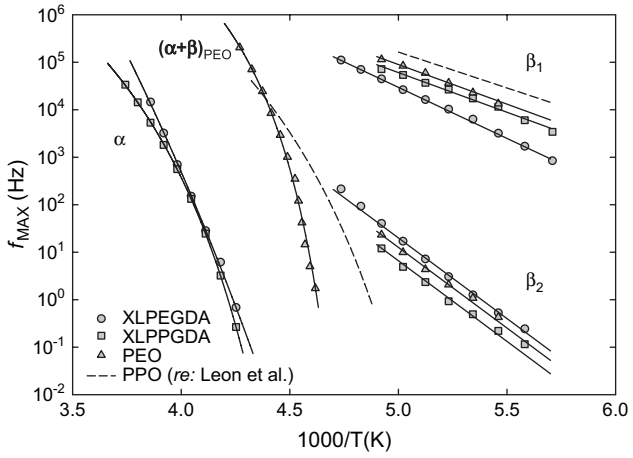

Fig. 8. Arrhenius plot of f_{MAX} (Hz) *vs.* $1000/T$(K) for XLPEGDA, XLPPGDA and PEO. Dashed lines correspond to data for PPO polymer [40].

relationship which is indicative of a local relaxation process; this behavior is typical of sub-glass relaxations in amorphous and semi-crystalline polymers [14,32]. The positions of the β_1 and β_2 relaxations in the crystalline PEO sample are virtually identical to those reported previously (*re*: γ and γ' processes, respectively [19]). The apparent activation energies (E_A) of the individual relaxations are reflected in the slope of the data for each material. For the β_1 relaxation, XLPEGDA displays an activation energy of 41 kJ/mol, as compared to 32 kJ/mol for the corresponding process in crystalline PEO; this difference in E_A for the β_1 process presumably reflects differences in the local relaxation environment experienced by the responding dipoles in the highly crosslinked network, as compared to motions originating from the amorphous regions within the PEO crystals. In XLPPGDA, the β_1 activation energy is also 32 kJ/mol. This value is nearly the same as values reported in the literature for the sub-glass relaxation in PPO polymer [40,41]; relaxation data for PPO reported by Leon et al. ($E_A = 29$ kJ/mol) [40] are included in Fig. 8 for comparison purposes. The close match in apparent activation energy between PPO and XLPPGDA is consistent with the wholly amorphous character of both PPO and the XLPPGDA network. For the β_2 relaxation, the time–temperature relation for all three materials can be described by a single activation energy, $E_A = 65$ kJ/mol.

Examination of the dielectric contour plots in Fig. 3, as well as the time–temperature results in Fig. 8, establishes the similarity in sub-glass relaxation behavior for PEO, XLPEGDA, and XLPPGDA. In all three cases, an intermediate "fast" relaxation process (β_2) is observed with a corresponding relaxation time that is much shorter than that associated with the glass transition. As discussed above, dielectric studies completed by Jin et al. on PEO show this same intermediate relaxation, the origin of which was assigned to non-cooperative motions in the vicinity of the crystal–amorphous interface [19]. It was suggested that the fast process corresponds to a subset of segmental motions that, owing to the confinement imposed by the crystalline lamellae, assume a more localized character. The resulting dipolar relaxation

process, which encompasses motions of lesser cooperativity, appears at lower temperature (*i.e.*, shorter relaxation time) and with an Arrhenius time–temperature profile more characteristic of a local relaxation. An analogy was drawn between the behavior observed in bulk PEO and the response of amorphous PEO chains confined between inorganic layers in an intercalated nanocomposite [20,21]. In a recent publication, Elmahdy and co-workers report the emergence of an intermediate "fast" process in PEO/silicate nanocomposites; the intensity of this process, which displays local Arrhenius character, correlates with the amount of PEO confined within the intercalated galleries [21]. It is conceivable that a comparable mechanism is operative in the XLPEGDA and XLPPGDA networks, with the constraint imposed by the crosslink junctions extending along the contour of the PEGDA or PPGDA bridging groups (see Fig. 1). This constraint could potentially be responsible for the β_2 process encountered in the networks, in the same way that the constraint experienced by the polymer chain segments in the vicinity of the crystal surface leads to the observed fast process in PEO.

3.4. Analysis of the glass–rubber relaxation

In the glass transition region, the dielectric spectra show overlap of the β and α relaxation processes as well as the influence of conduction (*re*: Fig. 3). HN analysis was performed across the frequency domain in the vicinity of T_g in order to deconvolute the individual dipolar relaxation processes, and to remove the influence of conduction. The governing expression in this region is as follows:

$$\varepsilon^* = \varepsilon' - \mathrm{i}\varepsilon'' = \varepsilon_{\mathrm{U}_1} + \sum_{i=1}^{2} \frac{\varepsilon_{\mathrm{R}_i} - \varepsilon_{\mathrm{U}_i}}{\left[1 + (i\omega\tau_{\mathrm{HN}_i})^{a_i}\right]^{b_i}} - i\left(\frac{\sigma}{\varepsilon_o \omega}\right)^N \qquad (2)$$

where σ is the conductivity and ε_o is the vacuum permittivity. For an ideal conduction process, N assumes a value of 1 [25].

Dielectric loss data and corresponding HN curve fits for XLPEGDA in the glass transition region are plotted in Fig. 9. The data are shown with the conduction contribution subtracted according to Eq. (2). For all temperatures examined, the conduction contribution could be satisfactorily described with a value of $N = 1$; *i.e.*, $\varepsilon''_{\mathrm{cond}}$ varied consistently with ω^{-1}. The data, and corresponding HN fits, display a strong overlap of the β and α relaxations in this temperature range. The relaxation times (τ_{MAX}) associated with the individual peak maxima were determined from the HN best-fit parameters according to the following equation [25]:

$$\tau_{\mathrm{MAX}} = \tau_{\mathrm{HN}} \left[\frac{\sin\left(\frac{\pi ab}{2+2b}\right)}{\sin\left(\frac{\pi a}{2+2b}\right)}\right]^{1/a} \qquad (3)$$

For the merged β relaxation ($\beta_1 + \beta_2$), the skewing parameter (b) was taken as equal to 1, so that $\tau^{\beta}_{\mathrm{MAX}} = \tau^{\beta}_{\mathrm{HN}}$. The frequency maxima for the separated α relaxation process, $f_{\mathrm{MAX}} = [2\pi\tau_{\mathrm{MAX}}]^{-1}$, were the basis for the data points plotted in Fig. 8 (XLPEGDA & XLPPGDA). In the case of PEO, the combined influence of MWS polarization and the strong overlap of the α and β relaxations made it impossible to reliably separate the data into their constituent dispersions. As a result, the values plotted in Fig. 8 for PEO correspond to f_{MAX} for the merged $\alpha + \beta$ process, after correction for conduction.

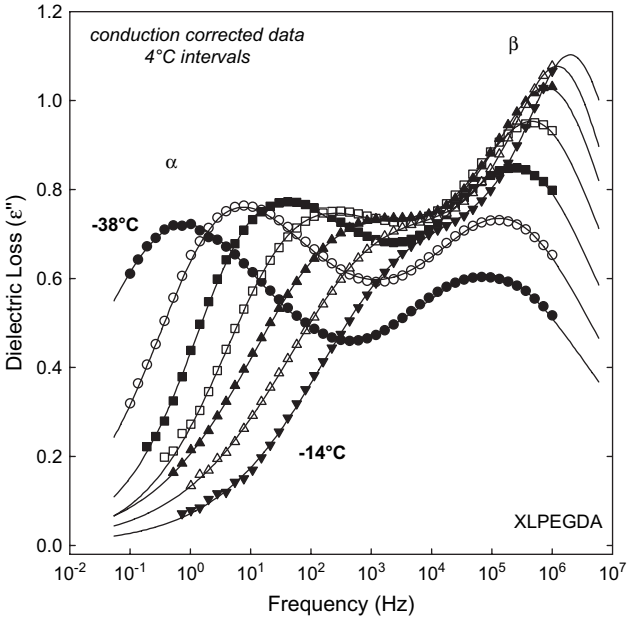

Fig. 9. Dielectric loss (ε'') *vs.* frequency (Hz) for XLPEGDA; temperatures from −38 °C to −14 °C at 4 °C intervals. Data are corrected for conduction contribution according to Eq. (2). Solid curves are dual HN fits.

Dielectric loss data for XLPPGDA in the α relaxation region are shown in Fig. 10. Since the β relaxation process in this network is very weak as compared to the α process, the spectra for XLPPGDA could be fit across the range using a single HN function, with the corresponding curves as shown.

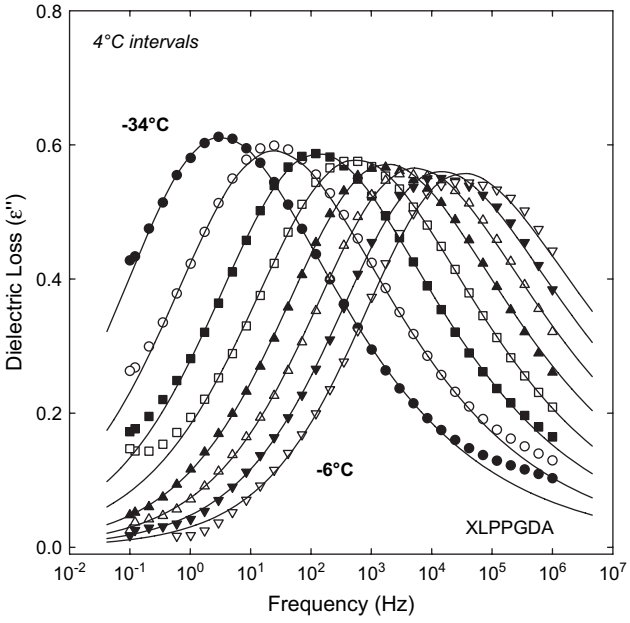

Fig. 10. Dielectric loss (ε'') *vs.* frequency (Hz) for XLPPGDA; temperatures from −34 °C to −6 °C at 4 °C intervals. Solid curves are HN fits.

The small influence of the β process, evident at high frequencies for the lower-temperature curves shown in Fig. 10, was removed by eliminating the effected points during the HN fit procedure. The resulting f_{MAX} values, derived from the HN fits and Eq. (3), are plotted in Fig. 8.

Examination of the α relaxation results for XLPEGDA and XLPPGDA in Fig. 8 show the relaxations offset to higher temperatures as compared to the experimental values for PEO and literature values for PPO [40], respectively; the positive offset for both networks is most likely the result of constraints imposed by network connectivity on the cooperative motions inherent to the α process. The non-Arrhenius time–temperature characteristics of the α relaxation are almost the same for both networks and can be described in the vicinity of T_g by the Vogel–Fulcher–Tammann (VFT) equation (see solid curves in Fig. 8) [47]. The near coincidence of the data points for XLPEGDA and XLPPGDA in Fig. 8 indicates a similar apparent activation energy or dynamic fragility associated with the underlying segmental motions occurring in both networks [48,49]. This result may reflect a trade-off between structural differences in the two networks, and their inherent free volume. While the motions in XLPEGDA would encompass segments that are fairly smooth and compact [50], the fractional free volume available for such motions is relatively low. By contrast, re-orientations encompassing the $-CH_3$ pendant group present in the XLPPGDA repeat unit would arguably require greater cooperativity, but motions involving this segment occur in a network with higher FFV. The net result appears to be time–temperature α relaxation characteristics that are nearly indistinguishable for these two particular networks.

A concise format for the comparison of dispersion characteristics (*i.e.*, relaxation intensity, shape) in XLPEGDA and XLPPGDA is the Cole–Cole plot. Cole–Cole plots of ε'' *vs.* ε' at −34 °C are shown in Fig. 11. For XLPEGDA, the α and β relaxations are broken into their constituent curves according to the HN fits. For the α process, the high frequency, asymmetric broadening associated with the HN form is observed, with a corresponding value of the skewing parameter, $b = 0.54$. A similar value was obtained for XLPPGDA, also at −34 °C. The merged sub-glass process is very prominent in XLPEGDA, while it appears only as a small shoulder in the XLPPGDA dispersion. Based on the data available for PPO, this latter result is perhaps not unexpected, as the sub-glass relaxation observed in the PPO polymer is quite weak relative to the glass transition [37,40,41]. However, if the "β_2" portion of the merged sub-glass process can be attributed to a subset of segmental motions that become faster and less cooperative as a result of confinement effects, it is somewhat surprising that the β process does not appear more prominently in the results for the XLPPGDA network. This is particularly noteworthy given that the network includes strongly dipolar ester linkages located at the crosslink junctions, moieties that could amplify the measured intensity of any segmental re-orientations

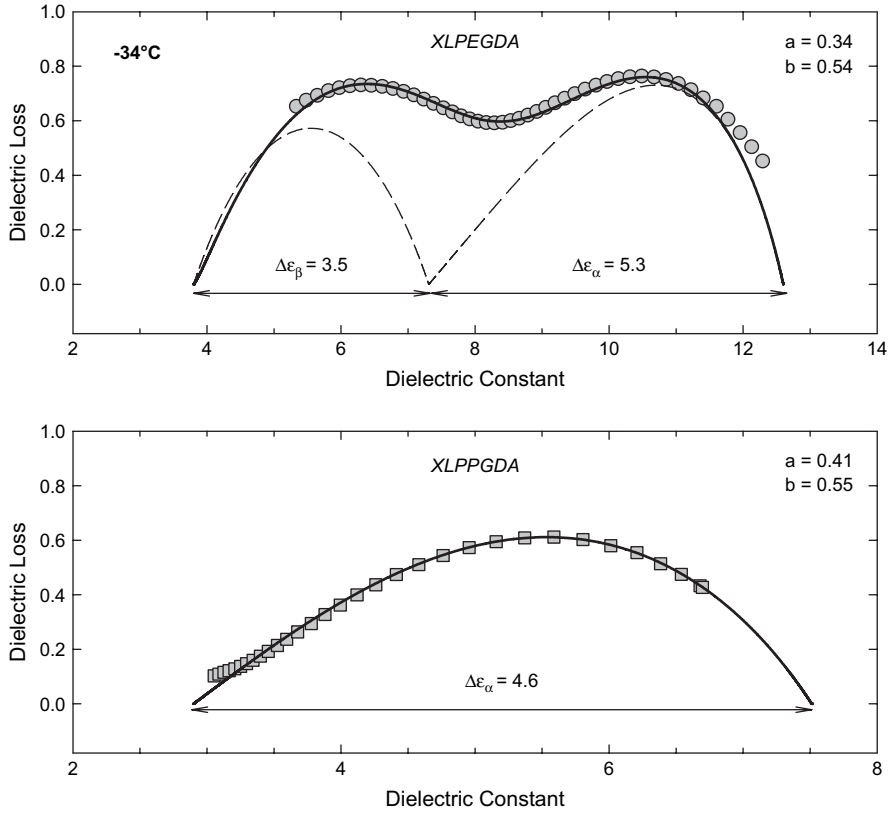

Fig. 11. Cole–Cole plots of dielectric loss (ε'') *vs.* dielectric constant (ε') for XLPEGDA and XLPPGDA at −34 °C. Solid curve is HN best fit. HN fit parameters (*a*,*b*) for the α relaxation are as indicated.

originating in the vicinity of the crosslinks. Apparently, while the constraint in XLPPGDA is sufficient to produce a measurable ''fast'' relaxation, the underlying motions associated with the β_2 process remain limited or strongly coupled, such that only a weak dispersion is detected.

In the case of XLPEGDA, review of the curves in Fig. 6 indicates a considerably stronger β_2 process compared to either XLPPGDA or PEO, both in absolute terms and on the basis of the relative intensities of the β_2 *vs.* β_1 peaks. The enhancement of the β_2 process in XLPEGDA as compared to PEO may reflect an additional contribution by the network ester groups to the relaxation intensity associated with the ''fast'' segmental process, a process that would most likely be sensitive to the character of the crosslink junctions and the degree of constraint that they impose. This added dipolar response could provide some explanation for the relative strength of the merged β process as shown in Fig. 11. It is difficult to draw a definitive conclusion in this regard, however, given the very different relaxation environment present in the amorphous XLPEGDA network, as compared to crystalline PEO.

4. Conclusions

The relaxation characteristics of amorphous crosslinked networks based on the UV photopolymerization of PEGDA and PPGDA have been investigated using broadband dielectric spectroscopy. Dielectric measurements on the XLPEGDA and XLPPGDA networks reveal the emergence of a ''fast'', non-cooperative segmental relaxation located intermediate to the sub-glass and glass–rubber processes traditionally reported for PEO and PPO. This fast process appears to be analogous to an intermediate relaxation detected previously in crystalline PEO [19], a result that was confirmed by our independent experimental studies on PEO films. In the case of PEO, it was proposed by Jin et al. that the fast process was the result of segmental constraint in the crystal–amorphous transition region. Owing to the limited conformational freedom of the polymer chain segments in this region, a more localized, largely non-cooperative process emerges, apparently as a subset of the cooperative segmental motions that constitute the glass transition. The dielectric relaxation characteristics of XLPEGDA and XLPPGDA are similar in many respects to those encountered in PEO, suggesting that a comparable constraint or confinement mechanism could be responsible for the detection of a fast segmental relaxation process in the crosslinked networks. The appearance of this additional process may be a general phenomenon in systems with a sufficient level of chemical or physical constraint, as it is observed in the amorphous XLPEGDA and XLPPGDA crosslinked networks, crystalline PEO, and in dielectric studies on PEO nanocomposites.

Acknowledgments

We are pleased to acknowledge support from the Kentucky Science and Engineering Foundation as per Grant Agreement KSEF-148-502-05-130 with the Kentucky Science and Technology Corporation. This study was also supported through a Major Research Equipment Grant awarded by the Office of the Vice President for Research at the University of Kentucky.

Activities at the University of Texas were supported in part by the Chemical Sciences, Geosciences and Biosciences Division, Office of Basic Energy Sciences, Office of Science, U.S. Department of Energy (Grant no. DE-FG02-02ER15362). However, any opinions, findings, conclusions, or recommendations expressed herein are those of the authors and do not necessarily reflect the views of the DOE. Partial support from the National Science Foundation under grant number CTS-0515425 is also acknowledged.

References

[1] Kohl A, Nielson R. Gas purification. 5th ed. Houston: Gulf Publishing Co.; 1997.
[2] Lin H, Freeman BD. J Membr Sci 2004;239:105–17.
[3] Lin H, Freeman BD. J Mol Struct 2005;739:57–74.
[4] Priola A, Gozzelino G, Ferrero F, Malucelli G. Polymer 1993;34:3653–7.
[5] Lin H, Kai T, Freeman BD, Kalakkunnath S, Kalika DS. Macromolecules 2005;38:8381–93.
[6] Lin H, Freeman BD. Macromolecules 2005;38:8394–407.
[7] Kalakkunnath S, Kalika DS, Lin H, Freeman BD. Macromolecules 2005;38:9679–87.
[8] Kalakkunnath S, Kalika DS, Lin H, Freeman BD. J Polym Sci Part B Polym Phys 2006;44:2058–70.
[9] Lin H, Van Wagner E, Swinnea JS, Freeman BD, Pas SJ, Hill AJ, et al. J Membr Sci 2006;276:145–61.
[10] Lin H, Freeman BD. Macromolecules 2006;39:3568–80.
[11] Lin H, Van Wagner E, Raharjo R, Freeman BD, Roman I. Adv Mater 2006;18:39–44.
[12] Lin H, Van Wagner E, Freeman BD, Toy LG, Gupta RP. Science 2006;311:639–42.
[13] Raharjo RD, Lin H, Sanders DF, Freeman BD, Kalakkunnath S, Kalika DS. J Membr Sci 2006;283:253–65.
[14] Kalika DS. Dielectric spectroscopy of crystalline polymers and blends. In: Nalwa HS, editor. Handbook of low and high dielectric constant materials and their applications, vol. 1. New York: Academic Press; 1999. p. 275–327.
[15] Mijovic J. Dielectric spectroscopy of reactive network-forming polymers. In: Kremer F, Schonhals A, editors. Broadband dielectric spectroscopy. Berlin: Springer-Verlag; 2003. p. 349–84.
[16] Roland CM. Macromolecules 1994;27:4242–7.
[17] Roland CM, Ngai KL, Plazek DJ. Comput Theor Polym Sci 1997;7:133–7.
[18] Schroeder MJ, Roland CM. Macromolecules 2002;35:2676–81.
[19] Jin X, Zhang S, Runt J. Polymer 2002;43:6247–54.
[20] Vaia RA, Sauer BB, Tse OK, Giannelis EP. J Polym Sci Part B Polym Phys 1997;35:59–67.
[21] Elmahdy MM, Chrissopoulou K, Afratis A, Floudas G, Anastasiadis S. Macromolecules 2006;39:5170–3.
[22] Colthup NB, Daly LH, Wiberley SE. Introduction to infrared and Raman spectroscopy. New York: Academic Press; 1975.
[23] Decker C, Moussa KJ. J Appl Polym Sci 1987;34:1603–18.
[24] Wunderlich B. Macromolecular physics, crystal melting, vol. 3. New York: Academic Press; 1980.
[25] Schonhals A, Kremer F. Analysis of dielectric spectra. In: Kremer F, Schonhals A, editors. Broadband dielectric spectroscopy. Berlin: Springer-Verlag; 2003. p. 59–98.
[26] Connor TM, Read BE, Williams G. J Appl Chem 1964;14:74–80.
[27] Ishida Y, Matsuo M, Takayanagi M. J Polym Sci Polym Lett Ed 1965;3:321–4.
[28] Porter CH, Boyd RH. Macromolecules 1971;4:589–94.

[29] Se K, Adachi K, Kotaka T. Polym J 1981;13:1009–17.
[30] Wintersgill MC, Fontanella JJ, Welcher PJ, Andeen CG. J Appl Phys 1985;58:2875–8.
[31] Fanggao C, Saunders GA, Lambson EF, Hampton RN, Carini G, Di Marco G, et al. J Polym Sci Part B Polym Phys 1996;34:425–33.
[32] McCrum NG, Read BE, Williams G. Anelastic and dielectric effects in polymeric solids. London: John Wiley and Sons; 1967.
[33] Hedvig P. Dielectric spectroscopy of polymers. New York: John Wiley and Sons; 1977.
[34] Williams G. Trans Faraday Soc 1965;61:1564–77.
[35] Beevers MS, Elliott DA, Williams G. Polymer 1980;21:13–20.
[36] Varadarajan K, Boyer RF. Polymer 1982;23:314–7.
[37] Johari GP. Polymer 1986;27:866–70.
[38] Schlosser E, Schonhals A. Prog Colloid Polym Sci 1993;91:158–61.
[39] Ichikawa K, MacKnight WJ, Nozaki R, Bose TK, Yagihara S. Polymer 1994;35:1166–70.
[40] Leon C, Ngai KL, Roland CM. J Chem Phys 1999;110:11585–91.
[41] Mattsson J, Bergman R, Jacobsson P, Borjesson L. Chain-length-dependent relaxation scenarios in an oligomeric glassforming system: from merged to well-separated α and β loss peaks. Phys Rev Lett 2003;90(7): 075702/1–4.
[42] Roland CM, Psurek T, Pawlus S, Paluch M. J Polym Sci Part B Polym Phys 2003;41:3047–52.
[43] Havriliak S, Negami S. J Polym Sci Polym Symp 1966;14:99–103.
[44] Havriliak S, Havriliak SJ. Dielectric and mechanical relaxation in materials. Cincinnati: Hanser; 1997.
[45] Cole KS, Cole RH. J Chem Phys 1941;9:341–51.
[46] Schonhals A. Dielectric properties of amorphous polymers. In: Runt JP, Fitzgerald JJ, editors. Dielectric spectroscopy of polymeric materials: fundamentals and applications. Washington: American Chemical Society; 1997. p. 81–106.
[47] Kremer F, Schonhals A. The scaling of the dynamics of glasses and supercooled liquids. In: Kremer F, Schonhals A, editors. Broadband dielectric spectroscopy. Berlin: Springer-Verlag; 2003. p. 99–129.
[48] Angell CA. J Non-Cryst Solids 1991;131–133:13–31.
[49] Bohmer R, Ngai KL, Angell CA, Plazek DJ. J Chem Phys 1993; 99:4201–9.
[50] Ngai KL, Roland CM. Macromolecules 1993;26:6824–30.